5206
5317
5323

CCD MODULATION TRANSFER FUNCTION

R. D. Nelson — Rockwell International

W. P. Waters — Rockwell International

ext 5570

ABSTRACT

After some general discussion of the modulation transfer function (MTF), the MTF is examined and compared to experimental data for several charge-coupled-devices. These devices include the delay line, imager, and transversal filter. Because of the possible significance to reducing output circuitry noise in CCD's, the transfer function and noise-generating fluctuations in the transfer function for double sampling is examined. It is shown that if the sampling pulse widths have appreciable fluctuation, the double sampling technique can lead to an increase rather than a decrease in device noise. The concept and predicted performance for the motion-compensation CCD imager is presented. This device has a larger MTF and better optical sensitivity than camera mode devices of comparable dimensions. It is observed that a few transfer functions can partially characterize several devices.

This paper derives the modulation transfer function (MTF) for the charge-coupled-device (CCD) after some general discussion of the function. The MTF for specific devices being built in our laboratory is then examined. These devices include the delay line, multiplexer, imager, and transversal filter.

The modulation transfer function (MTF) is the ratio of device output to input in a particular observation domain. In the frequency domain (which will be used in the following), the MTF relates the amplitude and phase of a sinusoidal output to the corresponding sinusoidal input signal. The argument gives the phase shift and the modulus gives the attenuation. Generally the normalization used is unity amplitude and zero argument at zero frequency. In the case of a linear system, the MTF is simply the Fourier transform of the impulse response function. If o(t) is the response of the linear system to input i(t), the MTF is given by equation 2, where upper case symbols indicate frequency domain representation of functions.

$$o(t) = \int h(t - t') \, i(t') \, dt' \qquad (1)$$

$$MTF = O(\omega)/I(\omega) = H(\omega) = \int h(t-t') e^{i\omega(t-t')} d(t-t') \qquad (2)$$

In the case of a sampled data system such as a CCD, a single input frequency gives rise to several output frequencies. These additional signals are multiples and sidebands of all of the multiples of the sampling frequency. Because the additional output signals represent no additional information, the MTF is calculated using the component of the output having the same frequency as the input. This definition is tenable in the case of narrow-band signals; that is, signals with bandwidth less than the Nyquist frequency. In the case of wide-band signals, the sidebands of harmonics of the sampling frequency (fold-over signals) give rise to distortion. This distortion in the case of wide-band signals must be considered in addition to the device frequency-dependent response. This can be an important consideration in the case of an optical input where the input signal cannot always conveniently be bandwidth-limited. Harmonics of the input signal frequency will be generated by nonlinearities in the device characteristics (viz., nonlinear transfer efficiency and a signal dependent input capacitance).

The device will be described by transfer efficiency per bit or cell (α) and the length in bits (M). The transfer efficiency at space-time point (x,t) is given by the ratio of the differences in cell charge population after and before charge transfer.[1,2]

$$\alpha(x,t) = \frac{dq_{out}(x,t)}{dq_{in}(x,t-1)} \quad (3)$$

The transfer inefficiency (ε) will be defined by the charge which fails to transfer successfully during one transfer period.

$$\varepsilon(x,t) = \frac{dq_{remaining}(x,t)}{dq_{in}(x,t-1)} \quad (4)$$

In the analysis to follow the small-signal limit is taken where transfer inefficiency is given by a constant which is independent of signal amplitude. This model has been previously considered by several others.[3,4] Because a fixed fraction of charge in a cell is not transferred during one transfer period, the charge in cell x at time t depends on all the charges which entered the device at earlier times ($t'<t$) and have propagated through cell x. If $q_0(x',t')$ is the charge introduced into cell x' of an M-bit CCD at time t', the charge in cell x at time t is given by the following.

$$q(x,t) = \sum_{x'=x}^{N} \sum_{t'=\infty}^{t} T(x,x',t,t')q_0(x',t') \quad (5)$$

where:

$$T(x,x',t,t') = \binom{t-t'-\delta_{x,M+1}}{x-x'-\delta_{x,M+1}} \alpha^{x-x'} \times \varepsilon^{t-t'+x'-x} \quad (6)$$

$$\binom{A}{B} = \frac{A!}{B!\,(A-B)!} \quad (7)$$

$$\delta x,p = \begin{cases} 1 & x = p \\ 0 & x \neq p \end{cases} \quad (8)$$

The Kronecker delta appears in the binomial coefficient because charge can reach the output of the device only by transfer and not nontransfer of charge. Note that the transfer matrix (T) contains the spatial and temporal causal relations for charge appearance in a cell.

DELAY LINE

Data is introduced into one end of the delay line and extracted from the other. The magnitude of the MTF is reduced by transfer inefficiency, the size of the data sampling interval during input, and finite operating frequency.

The current appearing at the device output at time t is the result of integrating an input signal current at an earlier time, propagating the resulting charge down the CCD and converting the charge into a representative output current via some output circuitry (typically a source follower fet). If the output current waveform is w(t) and the input current is $i_0(t)$, the output current of an M-bit delay line with delay time M times τ is:

$$i(t) = \frac{w(t)}{RC} \sum_{t'=\infty}^{t-M} T(M,0,t,t') \int_{t'}^{t'+\delta\tau} \times i_0(t'')dt'' \quad (9)$$

The data sampling interval is $\delta\tau$. The output waveform has been normalized by including the output capacitance C and the load impedance R. If a cosinusoidal input with frequency ω_o is considered, the Fourier transform of the output current is

$$I(\omega) = \lim_{T\to\infty} 1/T \int_0^T i(t)\, e^{i\omega t} dt \quad (10)$$

$$I(\omega) = \left\{ \sum_{p=-\infty}^{\infty} \delta(\omega \pm \omega_0 - \frac{2\pi p}{\tau}) \text{ X} \right.$$

$$\frac{W(\omega)\ T(\omega_0)\ i_0\ 2 \sin \omega_0 \delta\tau/2}{\omega RC} \text{ X}$$

$$\left. e^{i\omega_0(\delta\tau/2 - M\tau)} \right\} . \qquad (11)$$

where:

$W(\omega)$ = Fourier component of output waveform

$$= \frac{1}{\tau} \int_0^{\tau} w(t)\ e^{i\omega t} dt; \qquad (12)$$

$T(\omega_0)$= discrete Fourier transform of transfer matrix

$$= \sum_{t-t'=M}^{\infty} T(t-t')e^{i\omega_0(t-t')} \qquad (13)$$

$$= \left[1 + \frac{4\varepsilon \sin^2(\omega\tau/2)}{d^2} \right]^{-M/2} e^{-iM\psi} \qquad (14)$$

$$\cong e^{\frac{-2M\varepsilon}{\alpha^2} \sin^2(\omega\tau/2)} e^{-iM\psi} \qquad (15)$$

$$\psi = \tan^{-1}\left(\frac{\varepsilon \sin\omega\tau}{1-\varepsilon\cos\omega\tau}\right) \qquad (16)$$

Note that the spectrum consists of all of the harmonics of the transfer frequency and the concommitant sidebands. The spectral weight in the sidebands is predominantly due to the input waveform at frequencies below the Nyquist frequency and the output waveform for frequencies above the Nyquist frequency. The MTF is given by the spectral component of the Fourier transform having the same frequency as the input frequency. If for simplicity a sample-and-hold output circuit is considered, the MTF is:

$$M(\omega) = \frac{\sin\omega\tau/2}{\omega\tau/2} \frac{\sin\omega\delta\tau/2}{\omega\delta\tau/2} \text{ X}$$

$$\left[1 + \frac{4\varepsilon \sin^2\omega\tau/2}{(1-\varepsilon)^2} \right]^{-M/2} \text{ X}$$

$$e^{i\omega_0(\delta\tau/2 - \tau/2 - M\tau)} e^{iM\psi} \qquad (17)$$

The MTF decreases approximately exponentially with both device length in bits (M) and transfer inefficiency (ε). Note that transfer inefficiency has the maximum effect at the Nyquist frequency. The permissible values of device length & transfer inefficiency can be determined using equation (17) and the system requirements for a.c. gain ($|MTF|$) and phase shift. Figure 1 contains experimental measurements of the a.c. gain of a sixty-four bit shift register operating at twenty-five kilohertz. The solid line is the theoretical prediction using equation (17) and the crosses are experimental points.

DOUBLE SAMPLING

Ubiquitous 1/f noise, reset circuit noise, and other types of low frequency noise generated in the output circuitry can be removed using the technique of double sampling. Because of the possible significance to CCD's, the transfer function is described in the following paragraphs. In the double sampling technique, the output circuit signal measured prior to the integration of the CCD charge pulse is subtracted from the output circuit signal after integration of the CCD charge pulse. A small time spacing (t_0) between the two samples can cause large diminution of low-frequency noise. An uncertainty in the pulse widths (τ_p) employed in double sampling will imply a corresponding uncertainty in the transfer function and the sampled signal amplitudes. This noise introduced by imperfect double sampling can in some cases be greater than the noise reduction. If a single frequency (ω) component of noise with amplitude A is examined, the output signal and transfer function are given by the following:

$$I(\omega) = A\tau[e^{i\omega(t+t_0)} - e^{i\omega t}] \qquad (18)$$

$$= A\tau e^{i(\omega t+\omega t_0/2+\pi/2)} 2\sin(\omega t_0/2) \qquad (19)$$

$$M_{noise}(\omega) = e^{i(\omega t_0+\pi)/2} 2\sin(\omega t_0/2) \qquad (20)$$

If there is a fluctuation in the width of the sampling pulses, the mean square noise voltage referred to the output FET gate is given by

$$\langle\delta V^2\rangle_{fet} = \frac{\langle\delta\tau_p^2\rangle}{\langle\tau_p\rangle^2} \quad 2\langle\delta V_0^2\rangle+V_1^2+V_2^2 + 4A^2 \times$$

$$\sin^2(\omega t_0/2) + \langle\delta V^2\rangle_{CCD} \qquad (21)$$

where:

$\langle\delta\tau_p^2\rangle$ = mean square fluctuation in width of sampling pulse;

$\langle\delta V_0^2\rangle$ = mean square amplitude of output circuit noise voltage;

V_1 = first sample voltage;

V_2 = second sample voltage.

The first term of equation (21) arises from fluctuation of sampling pulse interval. The second term is the diminished output circuit noise and the final term is the noise arriving with the CCD charge packet. The first term can predominate in some cases because in the first term the rms noise-equivalent-charge is proportional to the number of signal charges and not the square root of the number of charges as is usually the case (term 3). The following is an example of poor double sampling.

CCD SIGNAL PARAMETERS

$q_{fat\ zero}$ = 20,000 carriers

q_{signal} = 500 carriers

$\langle\delta q^2\rangle^{\frac{1}{2}}_{CCD}$ = 200 carriers

$\langle\delta\tau^2\rangle^{\frac{1}{2}}_{\substack{output\\circuit}}$ = 200 carriers

$\dfrac{\langle\delta\tau_p^2\rangle^{\frac{1}{2}}}{\tau_p}$ = 0.02

case 1 - NO DOUBLE SAMPLING

$\frac{S}{N} = 1.77$

case 2 - DOUBLE SAMPLING

$\frac{S}{N} = 1.1$

TRANSVERSAL FILTER

In systems applications where low-level signals with large noise content are periodically generated, the signal-to-noise ratio can be improved by using a transversal filter with unit tap weights. Because of the application one might call the device a delay-and-add correlator. The transversal filter to be described is a CCD delay line with N inputs and n delay elements (bits) between input taps. The total device length is then n times N. The signal is time-sequentially applied to consecutive input taps. If the noise in different inputs is uncorrelated and the device has unity MTF, the signal emerging from the device will have a signal-to-noise improvement of $\sqrt{N}$. The MTF of this filter is reduced by transfer inefficiency, finite data sampling intervals, and timing-errors at the N inputs. In the following, the timing-error is expressed by a phase shift δ (between the signal propagating in the CCD and the input-tap signal) which occurs between consecutive inputs. The MTF is found by Fourier transforming the output signal resulting from a sinusoidal input.

$$M(\omega) = e^{i\omega(\delta\tau)/2} e^{-(N+1)x/2} \frac{\sinh Nx/2}{N \sinh x/2} \times$$

$$\frac{\sin\omega\tau/2}{\omega\tau/2} \frac{\sin\omega(\delta\tau)/2}{\omega(\delta\tau)/2} \qquad (22)$$

where:

$$x = \frac{2\varepsilon n}{\alpha^2} \sin^2(\omega\tau/2) + i(\psi-\delta); \qquad (23)$$

$$\psi = \tan^{-1}\left(\frac{\varepsilon \sin \omega\tau}{1-\varepsilon\cos\omega\tau}\right); \qquad (24)$$

δ = phase error between inputs;

τ = charge transfer period (1/operating frequency);

$\delta\tau$ = data sampling interval (generally one phase of transfer period).

Two instructive limits of this MTF are:

1. Phase shift limited (x is imaginary)

$$M = e^{i(\omega\delta\tau+(N+1)\delta)/2} \frac{\sin(\omega\delta\tau/2)}{\omega\delta\tau/2} \times$$

$$\frac{\sin(\omega\tau/2)}{\omega\tau/2} \frac{\sin(N\delta/2)}{N \sin(\delta/2)} \qquad (25)$$

2. Transfer efficiency limited (x is real)

$$M = e^{i(\omega\delta\tau-(N+1)\psi)/2} \frac{\sin\omega\delta\tau/2}{\omega\delta\tau/2} \times$$

$$\frac{\sin\omega\tau/2}{\omega\tau/2} e^{-(N+1)n\varepsilon\sin^2(\omega\tau/2)/\alpha^2} \times$$

$$\frac{\sinh(nN\varepsilon\sin^2(\omega\tau/2)/\alpha^2}{N\sinh(n\varepsilon\sin^2(\omega\tau/2)/\alpha^2} \qquad (26)$$

Case (1) shows the effect of errors in pulse timing and CCD operating frequency while Case (2) shows the effect of charge transfer inefficiency. Given the magnitudes of transfer inefficiency and timing-errors, the number of stages of filtering which maximizes the signal-to-noise ratio can be found. For comparison, the impulse gain for zero timing-error is:

$$g_I = e^{-Nn\varepsilon/2\alpha^2} \frac{\sinh(Nn\varepsilon/2\alpha^2)}{N\sinh(n\varepsilon/2\alpha^2)} \qquad (27)$$

IMAGER

A CCD can be used as an imager in a number of modes (i.e., frame transfer, line transfer, shuttered, unshuttered, interlaced, or non-interlaced). The construction of a number of these imagers has been reported in the literature.[5-9] In the following paragraphs, the MTF is examined for a one and a two-dimensional CCD imager. In addition, a new mode of operation is discussed. This new mode[10] (motion compensation) synchronizes the optical image motion and the CCD charge velocity. The synchronization allows the integration of a moving optical signal for a much longer period of time than the camera mode of operation and consequently greatly increases the optical sensitivity.

The CCD output lacks stationarity (invariance of image with respect to object motion) and as a result the MTF is not a local function of optical-object and electrical-image coordinates. This is the case because the distortion of a particular picture element depends upon the location of the imaging cell; the distortion becomes more severe as the imaging cell moves farther from the output end of the CCD. This difficulty might be resolved by specifying in the MTF the cell number of charge origin in addition to the spatial frequency of the optical input. Alternatively, because the signal is further degraded with each transfer, the worst case is considered by taking the cell number as the number of cells in the

CCD channel. The second suggestion will be used here.

The MTF for the charge-coupled-imaging-device is the product of functions accounting for the signal degradation due to thin film surface layer diffraction and refraction, diffusion of photogenerated carriers in the semiconductor bulk, carrier transit to and in the inversion layer, image motion, finite cell size, and transfer inefficiency in the readout process.

The surface layers affect quantum efficiency via transmissivity and absorption and MTF by near field diffraction of light by the gate lines and for non-zero incident light angles, multiple reflections in the surface thin film layers.

As an example of the effects of loss of MTF due to thin film multiple reflections, the optical point spread function of a single layer is given in a geometrical optics approximation

$$p(x-x_o) = \alpha e^{-\alpha|x-x_o|} \qquad (28)$$

where:

α= decay constant of point spread function

$$= \frac{\cot\theta}{t_\ell} \; m \left| \frac{(n_1+n_2)(n_2+n_3)}{(n_1-n_2)(n_2-n_3)} \right| ; \qquad (29)$$

θ= angle between light ray and the normal to the thin-film layer;

n_i= index of refraction of medium i;

t_ℓ= layer thickness.

As a crude approximation, the above formula is used to calculate the thin film contribution to the MTF $[M_o(k)]$.

$$M_o(k) = \frac{1}{\sqrt{1 + \frac{4\pi^2 k^2}{\alpha^2}}} \; e^{-i\tan^{-1} k/\alpha} \qquad (30)$$

The spatial frequency (k) is the reciprocal of the wavelength of the optical image. As a numerical example, the following constants are assumed:

$\theta = 35^o$ $\quad n_1 = 5$ $\quad n_3 = 5$

$k = .1\mu$ $\quad n_2 = 1.5$

The implied decay constant α is $3.5\mu^{-1}$ and the MTF is .66.

If the optical absorption length is comparable to or larger than the width of the depletion region, a considerable number of signal carriers will be generated in the semiconductor bulk. Because of the gradient in bulk minority carriers near the depletion region edge, the bulk photogenerated charge will diffuse to the surface and, as a result, improve the device quantum efficiency. However, in diffusing to the surface, charge also diffuses laterally, and, therefore, reduces the MTF. It is straight forward to show that the degradation of MTF due to bulk photo-generated charge is given by:

$$M_d = \left[1 - \frac{e^{-\alpha w}}{1 + \sqrt{\frac{\alpha^2}{(2\pi k)^2 + (1/L_d)^2}}} \right] \div \left[1 - \frac{e^{-\alpha w}}{1 + \alpha L_d} \right] \qquad (31)$$

where:

α = optical absorption coefficient;

L_d= bulk diffusion length;

w = mean depletion width.

From the above equation, it is apparent that the MTF is reduced when two conditions are met:

1. A large number of carriers are bulk photo-generated ($\alpha w \gtrsim 1$),

2. The wavelength of periodic input (divided by 2π) is less than both the diffusion length and absorption length ($\alpha < 2\pi k > 1/L_d$).

Both of these conditions are easily met in the near-infrared. The denominator of the above equation is the contribution to quantum efficiency due to recovery of bulk-generated charge. Note that, as would intuitively be expected, the quantum efficiency remains very good until the absorption length exceeds the diffusion length ($1./\alpha > L_d$).

The geometry of a line-array imager is shown in Figure 2. The cell length is L_c and the width is W_c. A fraction β of the cell length is photo-sensitive. Making less than the total cell length photo-sensitive raises the Nyquist frequency and the resolution capability of the device. The part of the cell length comprising the fraction β can be periodically varied for interlacing purposes.

The CCD is imagined to integrate a slowly moving optical image for a short time $\delta\tau$. The optical flux will be given by $J(x,t)$. The resulting charge is then transferred out of the device. The transfer process is described by transfer matrix $T_{nn'}$, where n and n$'$ are numbers labeling cells. The signal charge at the output fet (cell M + 1) is then

$$q(M+1) = \eta M_o M_d \sum_{n'} T_{M+1,n'} \int_{n'L_c}^{(n'+\beta)L_c} \quad X$$

$$dx' \int_0^{W_c} dy' \int_0^{\delta\tau} dt' J(x',y',t') \quad (32)$$

The quantum efficiency is given in the above equation by η. The MTF is found by the Fourier transform (now with respect to spatial variables).

$$M(k) = M_o M_d \, T(k) \, \frac{\sin(\pi k v \delta\tau)}{\pi k v \delta\tau} \quad X$$

$$\frac{\sin(\pi\beta k L_c)}{\pi\beta k L_c} \, e^{i\pi\beta k L_c}. \quad (33)$$

where:

v = optical image velocity;

k = spatial frequency;

$T(k)$= discrete Fourier transform of transfer matrix

$$= \left[1 + \frac{4\varepsilon \sin^2 \pi k L}{\alpha^2}\right]^{-M/2} e^{-iM\psi}. \quad (34)$$

The MTF obviously goes to zero for spatial frequencies twice the detector pitch and for integration times during which the image moves a spatial wavelength ($1/k$). The velocity (v) was assumed in the above to be in the channel direction and the spatial modulation was assumed to vary only in the channel direction (with no loss of generality). It should be pointed out that the $\sin(kx)/kx$ result is a well known result for a box type sensitivity function.

In discussing a two-dimensional array, it is more meaningful to make the spatial frequency a vector with direction given by the direction of maximum spatial modulation. Similarly, the optical image velocity will be a vector. It should be noted that these equations neglect fold-over of the input frequencies about the sampling frequency. In the case of optical images containing spatial wavelengths comparable to the detector pitch, these fold-over frequency components can lead to severe distortion.

The physics of the two-dimensional imaging array is almost identical to the line array case; however, the form of the MTF is more complicated because of the vector character of the variables. The result for charge transport in the x-direction is

$$M(k) = M_o M_d T(kx) \, \frac{\sin(\pi k \cdot Z_o)}{\pi k \cdot Z_o} \quad X$$

$$\frac{\sin(\pi k\cdot Z_1)}{\pi k\cdot Z_1}\ \frac{\sin\pi k\cdot Z_2}{\pi k\cdot Z_2}\ e^{-ik\cdot Z}. \qquad (35)$$

where:

$$Z = Z_o+Z_1+Z_2 \text{ (a 2-dimensional vector);} \qquad (36)$$

$$Z_o= \vec{v}\ \delta\tau; \qquad (37)$$

$$Z_1= \beta L_c\ \hat{x}\ ; \qquad (38)$$

$$Z_2= W_c\hat{y}\ ; \qquad (39)$$

In the laboratory in which the authors are employed, a new mode of CCD imager operation has been investigated. In the motion compensation mode,[10] the optical image is moved along the CCD array in synchronism with the channel charge, thus achieving a shutterless, highly sensitive sensor. The image impinging upon the CCD moves along the surface in a close approximation to the smooth image motion. In this way, the signal in one CCD cell can be built up over a considerable integration time without degrading the detector bandwidth or spatial frequency response. The enhancement in sensitivity is equal to the total integration time divided by the single cell sample time (τ).

Recognition that this device is a combination of a two-dimensional imager and the transversal filter previously described allows the MTF to be simply written down. Equation (35) for the MTF of an imager can be taken over directly with substitutions for the smearing time ($\delta\tau$) and transfer inefficiency smearing T(kx). The time interval during which motional smearing of the image takes place is the time required for the image to move over one gate (one phase of m- phase operation) of the CCD. The image smearing during charge propagation described by T(kx) in the two-dimensional imager was caused by transfer inefficiency. Allowance must now be made for mis-synchronization or dephasing of image velocity (v) and mean charge velocity (v_o). The mis-synchronization is expressed as a phase shift (δ) between electrical and optical signals in contiguous cells. The appropriate substitutions for the use of equation (35) are:

$$Z_o \rightarrow \vec{v}\beta L_c/m|v_o| \qquad (40)$$

$$T(kx) \rightarrow \frac{e^{in\gamma}}{n}\left[\frac{(1-A^n)^2+4A^n\sin^2 n\theta/2}{(1-A)^2+4A\ \sin^{-2}\theta/2}\right]^{\frac{1}{2}} \qquad (41)$$

where:

$$A^{-2}= 1 + \frac{4\varepsilon}{\alpha^2}\sin^2(\delta+\tau) \qquad (42)$$

$$\theta = \tan^{-1}\left(\frac{\sin\delta - \frac{\varepsilon}{\alpha}\sin\tau}{\cos\delta + \frac{\varepsilon}{\alpha}\cos\tau}\right) \qquad (43)$$

$$\gamma = \tan^{-1}\left[\frac{-A^n\sin n\theta+A\sin\theta + \ldots\ A^{n+1}\sin(n-1)\theta}{1-A^n\cos n\theta-A\cos\theta+\ldots\ A^{n+1}\cos(n-1)\theta}\right] \qquad (44)$$

$$\tau = 2\pi\beta k_x L_c \qquad (45)$$

$$\delta = 2\pi\vec{k}\cdot(\vec{v} - \vec{v}_o)\beta L_c/|v_o| \qquad (46)$$

n = number of in-track (x-direction) cells in the CCD

m = number of phases per CCD cell.

It is physically apparent that the larger the number of phases, the larger the MTF will be because of less motional smearing. Using four phases, the above equation gives an MTF at the Nyquist freuqency which is 97.5% of the MTF corresponding to an infinite number of phases (continuous charge motion). It is often the case that velocity mis-synchronization is more important than transfer inefficiency, the substitution for the charge propagation smearing function T(kx) then simplifies to

$$T(kx) \longrightarrow e^{in\delta}\ \frac{\sin n\delta/2}{n\delta/2} \qquad (47)$$

This simple expression gives the Q for velocity tuning of the motion compensating imager by adjustment of the drive frequency.

FIGURE 1

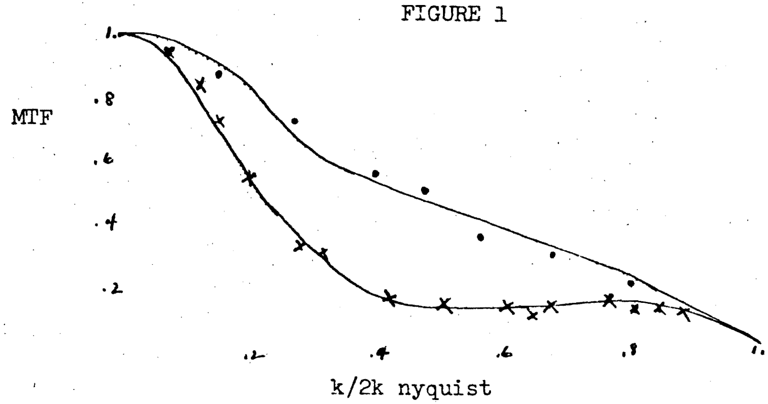

MTF for 64-Bit Delay Line. Upper curve ε=.013. Lower curve ε=.003. Solid Lines are theoretical predictions using the impulse to determine transfer inefficiency.

FIGURE 2

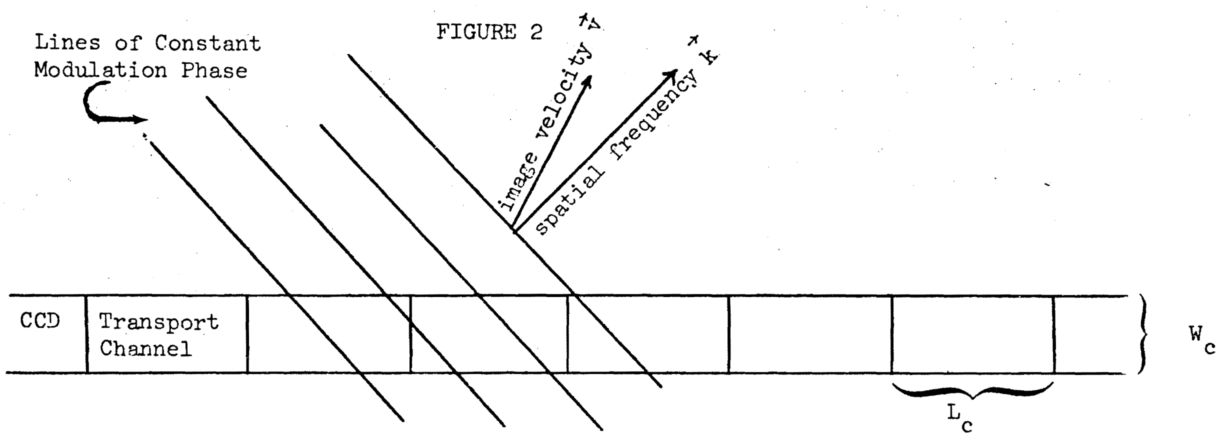

CCD Imager Device Geometry showing optical input superimposed on CCD transport channel. The direction of the spatial frequency vector is perpendicular to lines of constant phase.

SUMMARY

The MTF has been derived for several CCD applications. The MTF in these applications has been written as a product of functions, each accounting for an independent loss of modulation. All of the applications share some of the same sources of frequency-dependent signal diminution.

As in any sampled data system, the MTF decreases as the signal frequency approaches the Nyquist frequency. In addition, the MTF is reduced by a finite data-sampling aperture and transfer inefficiency. Transfer inefficiency was described by small-signal parameters and gave theoretical results in concert with experiment. Two algebraic forms describing transfer inefficiency sufficed for the applications considered. One form described the propagation of one signal down the entire device; the other form described an input signal which is periodically added to the channel signal at successive spatial points (using an input tap or an optical input). Transfer inefficiency was seen to have a maximum detrimental effect at the Nyquist frequency and no effect at zero frequency (where the MTF is unity), and at the sampling frequency (where the MTF is zero).

BIBLIOGRAPHY

1. W. S. Bayle and G. E. Smith, "Charge Coupled Semiconductor Devices," BSTJ, 49, 587 (1970).

2. C. Neil Berglund, and K. K. Thornber, "Incomplete Transfer in Charge-Transfer Devices," IEEE J. of Solid-State Circuits, SC-8, 108 (1973).

3. W. B. Joyce and W. J. Bertram, "Linearized Dispersion Relation and Green's Function for Discrete Charge Transfer Devices with Incomplete Transfer," BSTJ, 50, 1741 (1971).

4. G. F. Amelio, "Computer Modeling of Charge-Coupled-Device Characteristics," BSTJ, 51, 705 (1972).

5. M. G. Kovac, P. K. Weimer, F. V. Shallcross, and W. S. Pike, "Self-scanned Image Sensors Based Upon Bucket-Brigade Scanning," IEEE Devices Meeting Abstr., 106, October, 1970.

6. M. F. Tompsett, G. F. Amelio, W. J. Bertram, R. R. Buckley, W. J. McNamara, J. C. Mikkelsen, and D. A. Sealer, "Charge-Coupled Imaging Devices: Experimental Results," IEEE Trans. Electron Devices, ED-18, 992, (1971).

7. C. H. Siquin, D. A. Sealer, W. J. Bertram, M. F. Tompsett, R. R. Buckley, T. A. Shankoff, and W. J. McNamara, "A Charge-Coupled Area Image Sensor and Frame Store," IEEE Trans. Electron Devices, ED-20, 244, (1973).

8. S. G. Chamberlain, C. H. Chan, and D. R. Colton, "Self-Scanned Charge Coupled Optical Imaging Array," Presented at International Electron Devices Meeting, (IEEE), Washington, December 4-6, 1972.

9. M. H. White, D. R. Lampe, I. A. Mack, and F. C. Blaha, "CCD and Photosensitive Devices," Presented at the 1973 IEEE International Solid-State Circuits Conf., Philadelphia, PA, February, 1973.

10. Concept due to Dr. R. A. Gudmundsen, Rockwell International, Anaheim, CA.